PHYSICAL REVIEW A, VOLUME 65, 010703(R)

Simultaneous ionization-excitation of helium to $He^{+}(2p)$ magnetic sublevels by proton impact

H. Merabet, R. Bruch, and J. Hanni
Department of Physics, University of Nevada, Reno, Nevada 89557

A. L. Godunov and J. H. McGuire
Department of Physics, Tulane University, New Orleans, Louisiana 70118-5698

(Received 3 October 2001; published 12 December 2001)

Experimental magnetic substate cross section ratios σ_0/σ_1 and scattering angle-integrated cross sections following ionization-excitation of helium to $He^{+}(2p)\ ^2P^o$ in $H^{+}+He$ collisions have been determined, using polarization measurements of emitted radiation in the extreme ultraviolet region in combination with total cross sections, over a wide range of proton velocities (2–6 a.u.). These results are compared with second Born calculations fully including off-energy terms for the $He^{+}(2p)\ ^2P^o$ sublevels. We have found good agreement between theory and our He^{+} Lyman-α measurements.

DOI: 10.1103/PhysRevA.65.010703 PACS number(s): 34.50.Fa

Experimental observations of two-electron transitions such as double ionization, double excitation, and ionization-excitation have tested details of understanding of the time-dependent few-body problem, including the dynamics of electron correlation [1]. Recently, a theoretical description has been proposed [2,3], which separates time correlation from spatial correlation and predicts observable effects of time correlation. In the present paper, we report experimental magnetic sublevel cross sections [4,5], using extreme ultraviolet (EUV) spectropolarimetric techniques [6,7], namely high-resolution EUV spectrometry and intermediate resolution EUV polarimetry, of simultaneous ionization excitation to the $He^{+}(2p)\ ^2P^o$ state by intermediate- to-high-energy proton impact ($2<v<6$ a.u.). These measurements provide evidence for time correlation in the complex ionization-excitation dynamics of two electron target. In addition, our data for ionization of atomic He with concurrent excitation of a second electron into the three magnetic sublevels $M_L=0$ and $M_L=\pm1$ of the $2p$ excited state exhibits strong spatial electron correlation as well as quantum time ordering [8]. We also provide here clear evidence for time entanglement [2–3,9–10] between the two target electrons by comparing full second-order Born calculations with our spectropolarimetric experimental data. Furthermore, radiative emissions from singly charged ions such as He^{+} have been observed in solar spectra under solar-flare conditions [11]. Hence, the study of such complex nonequilibrium, anisotropic, beamlike systems may provide a deeper understanding of proton-induced jets in solar-flare astrophysical investigations.

The present paper focuses on the simultaneous ionization-excitation mechanism from the $He(1s^2)\ ^1S$ ground state to the final ionic state $He^{+}(2p)\ ^2P^0$ (also noted in this paper as $He\,\textsc{ii}\,(2p)^2P^o$) in $H^{+}+He$ collisions, followed by short wavelength radiative decay to the $He^{+}(1s)\ ^2S$ as follows,

$$H^{+}+He\rightarrow He^{+}(2p)\quad ^2P^o+e^{-}\rightarrow He^{+}(1s)^2S+h\nu \times(\lambda=30.4\ \text{nm}). \tag{1}$$

This process is difficult to investigate experimentally due to the very small EUV emission cross sections and theoretically because the electrons of the target are highly correlated. Until recently, only relative and/or absolute total cross-section measurements have been investigated [12–19]. Attempts to predict total and differential cross sections for the $H^{+}+He$ collisions include approximate first and second Born-type calculations for $He\,\textsc{ii}(2s)\ ^2S$ and $He\,\textsc{ii}\,(2p)\ ^2P^o$ states by Nagy and coworkers, Mezei *et al.*, and Osváth and Nagy [20–22] and Sidorovich [23]. However, these approximate calculations do not fully include off-shell terms in second Born, and they yield results that are lower than the experimental data. Amusia *et al.* and Bruch and coworkers [16,17] have also investigated theoretically the production of $He\,\textsc{ii}\,(2p)\ ^2P^o$ states for proton and electron impact. They have estimated the first- and second-order scattering contributions using semiempirical approaches and have found a strong Z_p^3 projectile charge dependence, which appears to represent quantum interference effects. In contrast, electron impact on helium was more thoroughly investigated [24–36] by means of double and triple total cross sections and magnetic substate populations. For example, Hayes, *et al.* [26] studied the polarization and alignment of the $He^{+}(2p)$ states by electron impact using coincidence techniques, whereas Götz *et al.* [27] measured the alignment of $He^{+}(2p)\rightarrow He^{+}(1s)+h\nu$ (30.4 nm) transition in the $e^{-}+He$ collision system using the angular distribution method. The first EUV degree of linear polarization measurements for $He\,\textsc{ii}$ Lyman-α and Lyman-β radiation following electron impact were performed by Bailey *et al.*, Merabet and coworkers, and McGuire *et al.* [6,7,9] using an EUV multilayer mirror (MLM) polarimeter.

In order to make relevant comparisons with theory, it is often necessary to perform experiments under conditions of absolute calibration of the experimental apparatus, or normalization procedures are devised to bring relative measurements onto an absolute scale. The uncertainties involved with absolute calibration or the normalization of relative measurements can present difficulties when comparing with theory or when comparing results from different investigators. One class of experiments, which are free from such problems, is polarization and angular distribution studies, which make use of relative intensity measurements. Furthermore, both polarization and angular distribution of the photons emitted by excited atoms and ions yield important information pertaining to the magnetic substate populations. The emitted radiation subsequent to the ionization-excitation process generally leads to a non-isotropic angular distribution, and polarization of the emitted light, owing to the nonuniform population of magnetic substates during the collision process.

In this paper, we have investigated the degree of linear polarization P subsequent to proton impact on helium. In our experiment, we have utilized cylindrical symmetric collisional geometry, Hence, P can be defined as,

$$P = \frac{I_{\parallel} - I_{\perp}}{I_{\parallel} + I_{\perp}}. \tag{2}$$

Here, $I_{\parallel}$ and $I_{\perp}$ are the intensities of radiation with electric-field vectors parallel and perpendicular with respect to the incident projectile beam direction when measured at an angle of 90°. The degree of linear polarization P is directly related to the sublevel cross-section ratios. Assuming LS coupling, where L and S are the orbital and spin angular momentum number of the excited levels, the degree of linear polarization for the He II$(2p)^2P^o$ state, can be expressed as [6,7]

$$P(^2P^o) = \frac{3(\sigma_0 - \sigma_1)}{7\sigma_0 + 11\sigma_1} = \frac{3(r-1)}{7r+11}, \tag{3}$$

where σ_{M_L} ($M_L = -1$, 0, and 1), are the magnetic sublevel angle-integrated excitation cross sections of specific M_L substates, $r = \sigma_0/\sigma_1$, is the cross-section ratio. Moreover, the total cross-section σ is the sum of the three magnetic sublevel cross sections,

$$\sigma = \sigma_0 + 2\sigma_1. \tag{4}$$

Thus, by combining Eq. (3) with Eq. (4), σ_{M_L} can be obtained for ionization-excitation process.

The experimental setup used in this paper consists of three main components: an ultra-compact EUV polarimeter; a 2 MV Van de Graaff accelerator, target cell and Faraday cup; and an intensity calibrated 1.5 m grazing incidence monochromator. A detailed description of this experimental setup is given elsewhere [6,7,18]. In brief, our lightweight ultra-compact polarimeter utilizes a molybdenum-silicon Mo/Si MLM device as a spectropolarimeter, optimized for a wavelength $\lambda = 30.4$ nm at an incidence angle of 50°, corresponding to the He II $(2p)^2P^o \rightarrow (1s)^2S$ transition. Our polarization measurements have been performed with a 10% VYNS spectral filter [6,7] that provides a transmission ratio of He I/He II line intensities of approximately 1000 000:1, so that the polarization measured with this filter contained approximately only a 1% contribution from the dominating He I (1 snp) $^1P^o$ radiative emission. Collisional deexcitation can also affect the observed radiation, leading to a redistribution of the magnetic substates between different levels. Consequently, a detailed pressure dependence of the emission from ionized-excited helium was obtained both with the 1.5 m grazing incidence monochromator and the polarimeter. To ensure a nondepolarization due to the target pressure for the Lyman-α of He II line, a target pressure of 0.03 Torr was selected. Furthermore, since magnetic fields can lead to a depolarization of the observed radiation by the Hanle effect, the gas cell used in this study was mounted inside a cylindrical magnetic shielding. With this shielding at the interaction region of the gas target a magnetic field smaller than 0.05 gauss was achieved. The corresponding total cross-sections σ measurements have been conducted using a 1.5 m high-resolution grazing incidence monochromator [18]. These results have been put on the absolute scale by renormalizing our proton data [18] to full second Born cross-section values presented in this paper for high-velocities impact ($v = 6.1$ a.u.). In addition, the obtained cross-section data have been corrected for alignment effects using [27],

$$\sigma(\theta) = \sigma \times \left\{ 1 + \frac{6P}{P-3} P_2(\cos\theta) \right\}, \tag{5}$$

where $\sigma(\theta)$ is the measured cross section, $\theta = 90°$ is the observation angle of the emitted photons, σ is the cross section for an isotropic distribution, $P_2(\cos\theta)$ is the second Legendre polynomial, and P is the degree of linear polarization. Statistics of the measured line intensities in this study were between 0.5 and 1% over most of the range of impact energies. Since the sum and difference of intensities are involved, the relative error of the polarization fraction increases rapidly with decreasing intensity. The relative error also becomes larger when the polarization fraction is small, reaching a maximum when it is close to zero. When instrumental uncertainties related to energy resolution of the Van de Graaff accelerator, target pressure stability, polarization, and charge normalization are combined, total uncertainty for magnetic scattering angle-integrated substate cross sections are found to be about 13 to 15% for He II$(2p)$ $^2P^o$ states. The current experimental He II$(2p)$ $^2P^0$ polarization results have not been corrected for cascade effects because the partial magnetic substate cross sections for the higher He II (nl) magnetic substates are not yet accurately known.

The magnetic sublevel cross sections for ionization-excitation of helium by proton impact have been calculated using an expansion of the transition amplitude in the Born series over the projectile-target interaction through the second order. The explicit equations can be found elsewhere [10]. The approximation level of the computational model was varied to explore the role of different kinds of mechanisms and interactions, especially the roles electron-electron correlation and off-shell energy terms. The off-shell energy terms give rise for time correlation between the two electrons [2,3,37]. There are similarities between correlation in space and correlation in time [2]. Both can be defined as a deviation from an uncorrelated limit. The uncorrelated limit is defined by a product form. The uncorrelated limit may also be described by an average of the appropriate correlation operator. In both the spatial and temporal cases, the average term can form the basis for useful approximate calculations. While correlation in space arises in the asymptotic target Hamiltonian and affects both the asymptotic wave function and the evolution operator, correlation in time can occur only

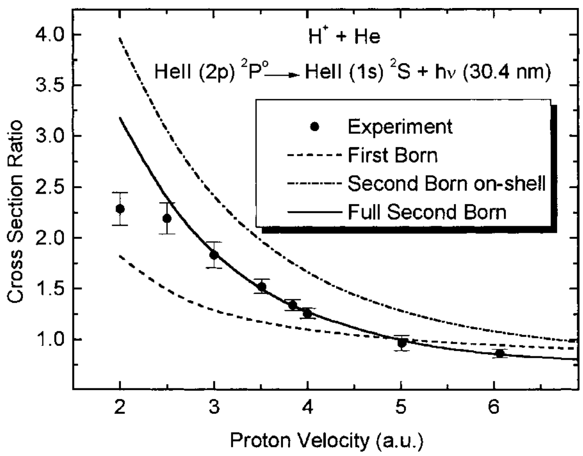

FIG. 1. Magnetic sublevel cross section ratios, $r=\sigma_0/\sigma_1$, for He II$(2p)^2P^o \rightarrow (1s)^2S$ radiation as function of proton velocity compared with first and second Born calculations. The full second Born calculation includes both on-shell and off-shell terms. The off-shell terms produce time correlation between electrons.

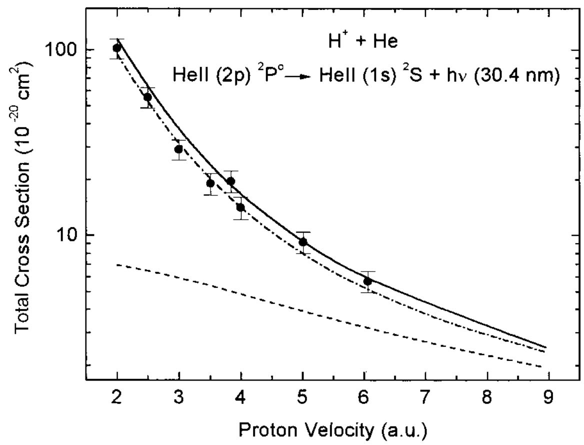

FIG. 2. Total cross sections for ionization-excitation to He II$(2p)^2P$ states by proton impact. Notations are the same as Fig. 1.

in the time evolution operator. Correlation in space comes from interelectron interactions within the target. Time correlation arises from time ordering of the external interactions.

In Fig. 1, we present the sublevel cross-section ratios σ_0/σ_1 as a function of the projectile velocity compared with our present theoretical results for He II$(2p)$ states. It is clear that a first-order theory does not accurately describe the energy dependence of these ratios. The second-order calculation obtained in the on-shell energy approximation, provides some improvement, but still does not completely agree with the data. Only the off-shell second-order calculation that fully includes both spatial and temporal correlation [2] is in agreement with our experimental results, except at the lowest energies shown. At these lowest energies, higher-order terms beyond second order are expected to be significant. Such findings give evidence of the presence of both correlation in space and correlation in time between electrons in $H^+ + He$ collisions for the ionization-excitation mechanism.

Figure 2 exhibits the observed $He^+(2p)$ total cross sections as well as first and second Born calculations. The first Born results are clearly too low, especially at the lower velocities. The second Born calculations, with and without off-shell contributions, are both in agreement with our data. The effect of the off-shell terms that produce time correlation between the electrons is to increase the cross sections by about 20% or so in this figure. The influence of the off-shell term is nearly constant for velocities up to 7 a.u., then gradually decreases with increasing the projectile velocity. It is evident in Fig. 2 that the first and second Born calculations converge at higher velocity.

Figure 3 shows the first experimental magnetic sublevel angle-integrated cross sections σ_0 and $\sigma_{\pm 1}$ for proton impact along with the results of our theoretical compilations. The behavior of the σ_0 and $\sigma_{\pm 1}$ cross sections is qualitatively similar to the total cross section for ionization-excitation. The second Born cross sections and the experimental data do not converge to the first Born result until the collision velocity is above 10 a.u. The effect of off-shell time correlation terms is to increase the second Born cross sections somewhat. We note that such a slowly varying effect is not typical for double excitation [3], but is typical of double ionization [1], except for the sign. We also note that the effect of the off-shell terms is greater in $\sigma_{\pm 1}$ than in σ_0. This means that the independent time approximation [2] is more sensible for the $M_L = \pm 1$ magnetic substate population $\sigma_{\pm 1}$ than for σ_0.

In conclusion, we have reported in this paper experimental magnetic sublevel angle-integrated cross-sections σ_0 and $\sigma_{\pm 1}$ for the $H^+ + He$ collision system at wide range of impact velocities. The excellent agreement of our full second Born calculations with our magnetic sublevel cross-section ratios has revealed the importance of temporal electron cor-

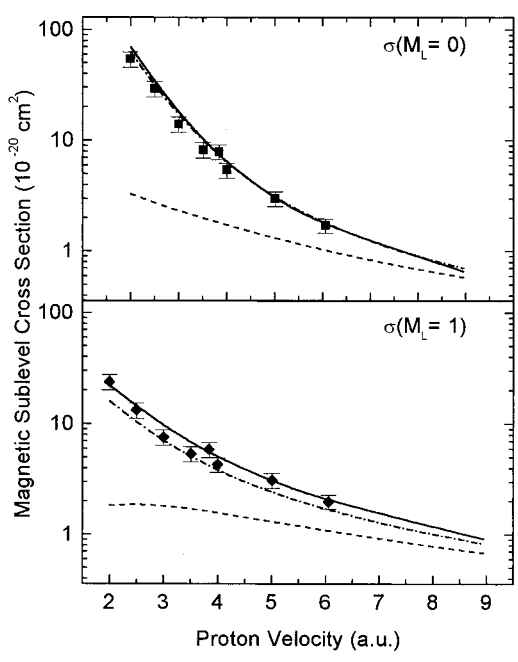

FIG. 3. Magnetic sublevel scattering angle-integrated cross sections for ionization excitation to He II$(2p)^2P^o$ states with $M_L=0$ (squares) and $M_L = \pm 1$ (diamonds) by proton impact. Notations for theory are the same as Fig. 1.

relation in the simultaneous ionization-excitation process. Furthermore, we used here this outstanding agreement to suggest benchmark theoretical results for absolute calibration of total cross sections, which may overcome the factor 2 or 3 deviation between the pioneering calculations [20,33] and previously observed measurements [18]. We have also shown in this paper that our polarization technique, when combined with EUV spectrometry, can evolve as a powerful tool for providing detailed information about the magnetic substate cross sections. Finally, the comprehensive data presented in this paper have important applications for the understanding of quantum phenomena such as time entanglement and are also significant for plasma diagnostics and astrophysical investigations such as solar flares.

This Project has been supported by ACSPECT Corporation and the Nevada Business and Science Foundation, (NBSF) Reno, Nevada and in part by Division of Chemical Sciences, Office of Sciences, U.S. Department of Energy.

[1] J. H. McGuire, *Electron Correlation Dynamics In Atomic Collisions* (Cambridge University, Cambridge, 1997).
[2] A. L. Godunov and J. H. McGuire, J. Phys. B **34**, L223 (2001).
[3] J. H. McGuire *et al.*, Phys. Rev. A **65**, 052706 (2001).
[4] U. Fano and H. Macek, Rev. Mod. Phys. **45**, 553 (1973).
[5] K. Bartschat, J. Phys. IV (P6) **9**, 17 (1999).
[6] M. Bailey *et al.*, Appl. Opt. **38**(19), 4125 (1999).
[7] H. Merabet *et al.*, Phys. Rev. A **60**, 1187 (1999).
[8] N. Solterfoht *et al.*, Phys. Rev. A **51**, 350 (1995).
[9] J. McGuire *et al.* (unpublished).
[10] A. L. Godunov *et al.*, J. Phys. B **30**, 3227 (1997).
[11] S. A. Kazantsev *et al.*, Opt. Spectrosc. **78**, 729 (1995).
[12] E. W. Thomas *et al.*, Phys. Rev. **164**, 143 (1967).
[13] E. Träbert, P. H. Heckmann, R. Bruch, and S. Fülling, Nucl. Instrum. Methods Phys. Res. B **23**, 155 (1987).
[14] J. O. Pedersen *et al.*, J. Phys. B **23**, 441 (1990).
[15] S. Fülling *et al.*, Phys. Rev. Lett. **68**, 3152 (1992).
[16] M. Ya. Amusia, E. A. Rauscher, R. Bruch, and S. Fülling, Nucl. Instrum. Methods Phys. Res. B **79**, 117 (1993).
[17] R. Bruch *et al.*, J. Phys. B **26**, L143 (1993).
[18] M. Bailey *et al.*, J. Phys. B **28**, 2655 (1995).
[19] K.-H. Schartner *et al.*, J. Phys. B **24**, L13 (1991).
[20] L. Nagy *et al.*, Phys. Rev. A **52**, R902 (1995).
[21] J. Mezei *et al.*, Nucl. Instrum. Methods Phys. Res. B **154**, 295 (1999).
[22] Z. Osváth and L. Nagy, Phys. Lett. A **271**, 385 (2000).
[23] V. A. Sidorovich, J. Phys. B **30**, 2187 (1997).
[24] H. R. Moustafa Moussa *et al.*, Physica (Amsterdam) **36**, 646 (1967).
[25] J. L. Forand *et al.*, J. Phys. B **18**, 1409 (1985).
[26] P. A. Hayes *et al.*, Phys. Rev. Lett. **77**, 3098 (1996).
[27] A. Götz *et al.*, J. Phys. B **29**, 4699 (1996).
[28] B. Rouvellou *et al.*, J. Phys. B **33**, L599 (2000).
[29] M. Dogan *et al.* and references therein, J. Phys. B **31**, 1611 (1998).
[30] M. R. H. Rudge, J. Phys. B **21**, 1887 (1988).
[31] A. V. Kuplyauskene *et al.*, Opt. Spectrosc. **71**, 127 (1991).
[32] A. Raeker *et al.*, J. Phys. B **27**, 3129 (1994).
[33] A. Franz and P. L. Altick, J. Phys. B **28**, 4639 (1995).
[34] P. J. Marchalant *et al.* and references therein, J. Phys. B **31**, 1141 (1998).
[35] P. J. Marchalant *et al.*, J. Phys. B **33**, L749 (2000).
[36] Y. Fang *et al.*, J. Phys. B **34**, L19 (2001).
[37] J. H. McGuire *et al.*, J. Mass Spectrom. **192**, 65 (1999). The Fourier transform of the off-energy-shell term, $P_v 1/(E-E')$, in the energy space propagator generates time correlation, namely, $\theta(t)-\theta_{\mathrm{av}}$, in time propagation. Here, P_v is the principal value term which excludes the energy conserving singularity at $E'=E$, and $\theta(t)-\theta_{\mathrm{av}}$ is the Heavyside step function minus its time averaged value.